EPJ Web of Conferences **175**, 05009 (2018) https://doi.org/10.1051/epjconf/201817505009
Lattice 2017

Baryon interactions from lattice QCD with physical quark masses – Nuclear forces and ΞΞ forces –

Takumi Doi[1,2,⋆], *Takumi* Iritani[1], *Sinya* Aoki[1,3,4], *Shinya* Gongyo[1], *Tetsuo* Hatsuda[1,2], *Yoichi* Ikeda[1,5], *Takashi* Inoue[1,6], *Noriyoshi* Ishii[1,5], *Takaya* Miyamoto[1,3], *Hidekatsu* Nemura[1,5], and *Kenji* Sasaki[1,3]

[1] *Theoretical Research Division, Nishina Center, RIKEN, Wako 351-0198, Japan*
[2] *iTHEMS Program and iTHES Research Group, RIKEN, Wako 351-0198, Japan*
[3] *Center for Gravitational Physics, Yukawa Institute for Theoretical Physics, Kyoto University, Kyoto 606-8502, Japan*
[4] *Center for Computational Sciences, University of Tsukuba, Tsukuba 305-8577, Japan*
[5] *Research Center for Nuclear Physics (RCNP), Osaka University, Osaka 567-0047, Japan*
[6] *Nihon University, College of Bioresource Sciences, Kanagawa 252-0880, Japan*

Abstract. We present the latest lattice QCD results for baryon interactions obtained at nearly physical quark masses. $N_f = 2 + 1$ nonperturbatively $O(a)$-improved Wilson quark action with stout smearing and Iwasaki gauge action are employed on the lattice of $(96a)^4 \simeq (8.1\text{fm})^4$ with $a^{-1} \simeq 2.3$ GeV, where $m_\pi \simeq 146$ MeV and $m_K \simeq 525$ MeV. In this report, we study the two-nucleon systems and two-Ξ systems in ${}^1S_0$ channel and ${}^3S_1$-${}^3D_1$ coupled channel, and extract central and tensor interactions by the HAL QCD method. We also present the results for the $N\Omega$ interaction in ${}^5S_2$ channel which is relevant to the $N\Omega$ pair-momentum correlation in heavy-ion collision experiments.

1 Introduction

In quest of the coherent unification of physics in different hierarchies, the baryon interactions serve as "the bridge from quarks to nuclei and cosmos" (particle-, nuclear- and astro- physics) [1]. Nuclear forces and hyperon forces govern the properties of (hyper) nuclei, and have been the subject of intensive theoretical/experimental investigations. These interactions also play a crucial role in the equation of state (EoS) of high dense matter, which is realized at the core of neutron stars. The recent observation of the binary neutron star merger [2, 3], which opens the new era of multi-messenger astronomy, certainly adds new urgency to the determination of baryon interactions.

In view of the importance of the first-principles calculations of baryon forces, we started the first realistic lattice QCD (LQCD) calculation of baryon interactions at nearly physical quark masses about two years ago, where the interaction kernels (so-called "potentials") are determined by the HAL QCD method [4, 5]. New challenges which are inherent in multi-baryon systems on a lattice are overcome by novel theoretical/algorithmic developments, most notably by (i) the time-dependent formalism of the HAL QCD method [6], (ii) the extension to coupled channels systems [7] and (iii) the unified

⋆Speaker, e-mail: doi@ribf.riken.jp

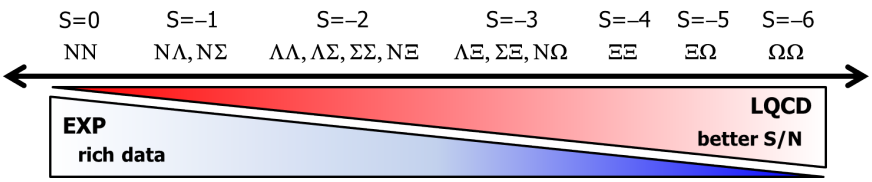

Figure 1. Illustrative figure for the complementary role of lattice QCD and experiments in the determination of baryon forces. Lattice QCD has a special strength to predict interactions in larger strangeness $|S|$ sectors, where experimental information is scare.

contraction algorithm [8]. In particular, time-dependent HAL QCD method enables us to extract baryon interactions without relying on the ground state saturation [6]. This is the indispensable feature for a reliable LQCD calculation of baryon interactions, since a typical excitation energy in multi-baryon systems is one to two orders of magnitude smaller than $O(\Lambda_{\rm QCD})$ due to the existence of elastic excited states. This is in contrast to the traditional approach (so-called "direct" calculations [9–11]), which relies on the ground state saturation and thus is generally unreliable [12–14]. The existence of uncontrolled systematic errors in the results of the previous direct calculations was explicitly exposed by the "sanity (consistency) check" proposed in Ref. [13].

Our aim in this first physical point calculation is the comprehensive determination of two-baryon interactions from the strangeness $S = 0$ to -6 (nuclear forces and hyperon forces) in parity-even channels. As is well known, the statistical fluctuations in LQCD are smaller (larger) for larger (smaller) quark masses, and thus the results have better precision in larger strangeness $|S|$ sector. On the other hand, an experiment in larger $|S|$ sector is more difficult due to the short life time of hyperons. Therefore, LQCD studies and experiments are complementary with each other in the determination of baryon forces (See Fig. 1). Our LQCD prediction on the "most strange dibaryon" ($\Omega\Omega$) system is already available in Ref. [15].

In this paper, we present the latest LQCD results for two-Ξ ($\Xi\Xi$) forces ($S = -4$) and two-nucleon (NN) forces ($S = 0$) in parity-even channel, updating our previous results [16]. Central forces are extracted in ${}^1S_0$ channel, and central and tensor forces are obtained in ${}^3S_1$-${}^3D_1$ coupled channel analysis. The results for other interactions between two octet baryons are presented in Refs. [17]. Interactions between decuplet and octet baryon also attract great interest and we have found that the $N\Omega$ system in ${}^5S_2$ channel is attractive strong enough to form a bound state at heavy quark masses [18]. In this report, we present the first physical point results of the $N\Omega$ (${}^5S_2$) interaction, which can be examined through the $N\Omega$ correlation in relativistic heavy-ion collision [19].

2 Formalism

In the HAL QCD method, the key quantity is the equal-time Nambu-Bethe-Salpeter (NBS) wave function. In the case of the NN system, for instance, it is defined by $\phi_W^{NN}(\vec{r}) \equiv 1/Z_N \cdot \langle 0|N(\vec{r},0)N(\vec{0},0)|NN,W\rangle_{\rm in}$, where N is the nucleon operator with its wave-function renormalization factor $\sqrt{Z_N}$ and $|NN,W\rangle_{\rm in}$ denotes the asymptotic in-state of the NN system at the total energy of $W = 2\sqrt{k^2+m_N^2}$ with the asymptotic momentum k, and we consider the elastic region, $W < W_{\rm th} = 2m_N + m_\pi$. The most important property of the NBS wave function is that the information of the phase shift $\delta_l(k)$ (l: the orbital angular momentum) is encoded in the asymptotic behavior at $r \equiv |\vec{r}| \to \infty$ as $\phi_W^{NN}(\vec{r}) \propto \sin(kr - l\pi/2 + \delta_l(k))/(kr)$. Exploiting this feature, one can define non-

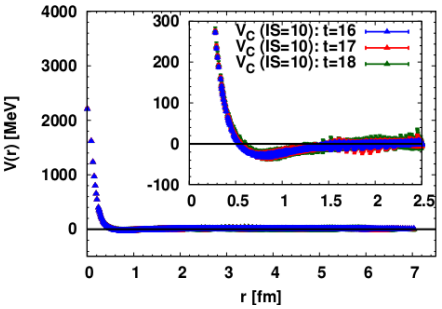

Figure 2. ΞΞ central force $V_C(r)$ in ${}^1S_0$ ($I = 1$) channel obtained at $t = 16 - 18$.

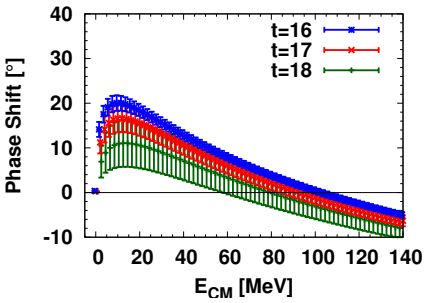

Figure 3. ΞΞ phase shifts in ${}^1S_0$ ($I = 1$) channel obtained at $t = 16 - 18$.

local but energy-independent potential, $U^{NN}(\vec{r}, \vec{r'})$, which is faithful to the phase shifts through the Schrödinger equation [4–6], $(E_W^{NN} - H_0)\phi_W^{NN}(\vec{r}) = \int d\vec{r'} U^{NN}(\vec{r}, \vec{r'})\phi_W^{NN}(\vec{r'})$, where $H_0 = -\nabla^2/(2\mu)$ and $E_W^{NN} = k^2/(2\mu)$ with the reduced mass $\mu = m_N/2$.

Generally speaking, the NBS wave function can be extracted from the four-point correlator, $G^{NN}(\vec{r}, t) \equiv \sum_{\vec{R}} \langle 0|(N(\vec{R} + \vec{r})N(\vec{R}))(t)\ \overline{(NN)}(t = 0)|0\rangle$, by isolating the contribution from each energy eigenstate (most typically by the ground state saturation with $t \to \infty$). Such a procedure, however, is practically almost impossible, due to the existence of nearby elastic scattering states. In fact, the typical excitation energy is as small as $O(1) - O(10)$ MeV, which is estimated by the empirical binding energies and/or the discretization in spectrum by the finite volume, $\sim (2\pi/L)^2/m_N$. Correspondingly, ground state saturation requires $t \gtrsim O(10) - O(100)$ fm, which is far beyond reach considering that signal/noise (S/N) is exponentially degraded in terms of t.

This fundamental problem inherent in multi-baryon systems on a lattice can be overcome by the time-dependent HAL QCD method [6], in which the signal of $U^{NN}(\vec{r}, \vec{r'})$ is extracted even from elastic excited states, using the energy-independence of $U^{NN}(\vec{r}, \vec{r'})$. More specifically, the following "time-dependent" Schrödinger equation holds even without the ground state saturation,

$$\left(-\frac{\partial}{\partial t} + \frac{1}{4m_N}\frac{\partial^2}{\partial t^2} - H_0\right) R^{NN}(\vec{r}, t) = \int d\vec{r'} U^{NN}(\vec{r}, \vec{r'}) R^{NN}(\vec{r'}, t), \tag{1}$$

where $R^{NN}(\vec{r}, t) \equiv G^{NN}(\vec{r}, t)e^{2m_N t}$. While it is still necessary to suppress the contaminations from inelastic states, it can be fulfilled by much easier condition, $t \gtrsim (W_{\rm th} - W)^{-1} \sim O(1)$ fm. This is in contrast to the direct calculations [9–11] which inevitably rely on the ground state saturation: They are generally unreliable due to the fake (mirage) plateau identification [12–14], and explicit evidences of the uncontrolled systematic errors were also exposed by the "sanity (consistency) check" given in [13].

3 Lattice QCD setup

$N_f = 2 + 1$ gauge configurations are generated on the 96^4 lattice with the Iwasaki gauge action at $\beta = 1.82$ and nonperturbatively $O(a)$-improved Wilson quark action with $c_{sw} = 1.11$ and APE stout smearing with $\alpha = 0.1$, $n_{\rm stout} = 6$. About 2000 trajectories are generated after the thermalization, and preliminary studies show that $a^{-1} \simeq 2.333$ GeV ($a \simeq 0.0846$ fm) and $m_\pi \simeq 146$ MeV, $m_K \simeq 525$ MeV. The lattice size, $La \simeq 8.1$ fm, is sufficiently large to accommodate two baryons on a box. For further details on the gauge configuration generation, see Ref. [20].

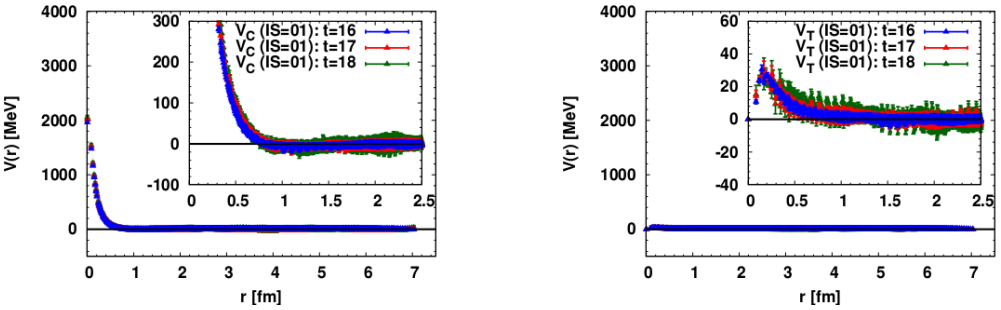

Figure 4. ΞΞ central force $V_C(r)$ (left) and tensor force $V_T(r)$ (right) in ${}^3S_1$-${}^3D_1$ ($I = 0$) channel obtained at $t = 16 - 18$.

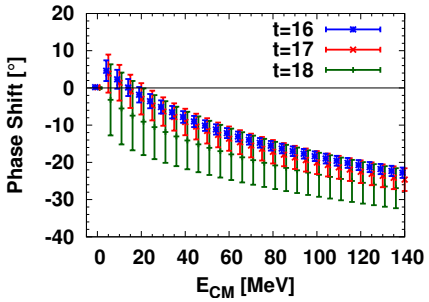

Figure 5. ΞΞ phase shifts in effective ${}^3S_1$ ($I = 0$) channel obtained at $t = 16 - 18$.

The measurements of NBS correlators are performed at the unitary point, where the block solver [21] is used for the quark propagator and unified contraction algorithm [8] is used for the contraction. The computation for the measurements (including I/O) achieves $\sim 25\%$ efficiency, or ~ 65 TFlops sustained on 2048 nodes of K computer. We employ wall quark source with Coulomb gauge fixing, where the periodic (Dirichlet) boundary condition is used for spacial (temporal) directions and forward and backward propagations are averaged to reduce the statistical fluctuations. We pick 1 configuration per each 5 trajectories, and we make use of the rotation symmetry to increase the statistics. The total statistics for NN and ΞΞ systems amounts to 414 configurations $\times$ 4 rotations $\times$ 72 wall sources binned by 46 configurations, and one for $N\Omega$ system is 200 configurations $\times$ 4 rotations $\times$ 48 wall sources binned by 10 configurations.

Baryon forces are determined in ${}^1S_0$ and ${}^3S_1$-${}^3D_1$ channels for NN and ΞΞ and in ${}^5S_2$ channel for $N\Omega$. We perform the velocity expansion [5] in terms of the non-locality of potentials, and obtain the leading order potentials, i.e., central and tensor forces. $N\Omega$ (${}^5S_2$) interaction is obtained neglecting the couplings to two octet baryons (e.g., ΛΞ) which are kinematically suppressed by the D-wave nature. In this preliminary analysis shown below, the term which corresponds to the relativistic effects ($\partial^2/\partial t^2$-term in Eq. (1)) is neglected.

4 ΞΞ systems ($S = -4$ channel)

We first present the results for the ΞΞ system in ${}^1S_0$ (iso-triplet) channel. This channel belongs to the 27-plet in flavor SU(3) classification as does the $NN({}^1S_0)$ system. Since the "dineutron" ($NN({}^1S_0)$)

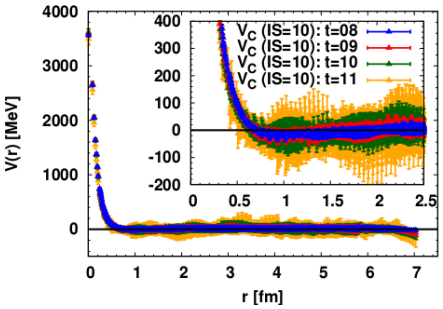

Figure 6. *NN* central force $V_C(r)$ in ${}^1S_0$ ($I = 1$) channel obtained at $t = 8 - 11$.

is nearly bound due to the strong attraction, it has been a long standing question whether or not the 27-plet interaction with the SU(3) breaking effects forms a bound $\Xi\Xi({}^1S_0)$ state [22].

Shown in Fig. 2 is the LQCD result for the central force $V_C(r)$ in the $\Xi\Xi({}^1S_0)$ channel. We observe a clear signal of the mid- and long-range attraction as well as the repulsive core at short-range, resembling the phenomenological potential in $NN({}^1S_0)$ system. Within statistical fluctuations, the results are found to be consistent with each other in the range $t = 16 - 18$, which suggests that the contaminations from inelastic excited states are suppressed and higher-order terms in the velocity expansion are small. In Fig. 3, we show the phase shifts in terms of the center-of-mass energy. It is found that the interaction is strongly attractive at low energies, while it is not sufficient to form a bound $\Xi\Xi({}^1S_0)$ state. Such a strong attraction may be observed by, e.g., heavy-ion collision experiments.

We next consider the $\Xi\Xi$ system in ${}^3S_1$-${}^3D_1$ (iso-singlet) coupled channel. This channel belongs to the 10-plet in flavor SU(3), a unique representation with hyperon degrees of freedom. By solving the coupled channel Schrödinger equation, the central and tensor forces are obtained, which are shown in left and right panels in Fig. 4, respectively. The strong repulsive core is observed in the central force, which can be understood from the viewpoint of the quark Pauli blocking effect [5, 23]. There also exists an indication of a weak attraction at mid range which may reflect the effect of small attractive one-pion exchange potential (OPEP). The $\Xi\Xi$ tensor force is found to be weaker with an opposite sign compared to the *NN* tensor force (right panel of Fig. 7). This could be understood by the phenomenological one-boson exchange potentials, where η gives weaker and positive tensor forces and π gives much weaker and negative tensor forces. We also calculate the effective central potential in ${}^3S_1$ channel by solving the (S-wave) single channel Schrödinger equation. The effects of the tensor force are implicitly included as ${}^3S_1 \to {}^3D_1 \to {}^3S_1$. The corresponding phase shifts in effective ${}^3S_1$ channel are given in Fig. 5, which reflect the repulsive nature of the interaction.

5 *NN* systems ($S = 0$ channel)

We present the results for the *NN* system in ${}^1S_0$ (iso-triplet) channel. In Fig. 6, we show the central force $V_C(r)$ obtained at $t = 8 - 11$. While the results suffer from large statistical fluctuations, the repulsive core at short-range is clearly observed. Its magnitude is more enhanced compared to that in $\Xi\Xi({}^1S_0)$, which can be understood from the one-gluon exchange picture. We also observe that the potential is attractive at mid- and long-range, resembling the phenomenological potential as OPEP. In order to suppress the contaminations from inelastic states, it is desirable to take larger t, while the statistical fluctuations become larger. Further studies with larger statistics are currently underway.

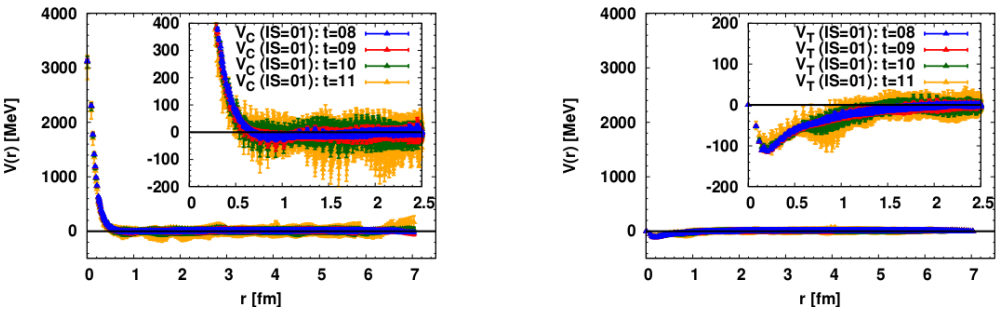

Figure 7. NN central force $V_C(r)$ (left) and tensor force $V_T(r)$ (right) in ${}^3S_1$-${}^3D_1$ ($I = 0$) channel obtained at $t = 8 - 11$.

We next consider the ${}^3S_1$-${}^3D_1$ (iso-singlet) channel. In the left and right panels of Fig. 7, we show the central force $V_C(r)$ and tensor force $V_T(r)$, respectively. The most notable observation is the strong tensor force with the long-range tail structure. Compared to the lattice tensor forces obtained with heavier quark masses [5], the range of interaction is found to be longer. In the central force, the repulsive core at short-range as well as mid- and long-range attraction are observed. Compared to the results of NN (${}^1S_0$) channel, there is a tendency that the interaction is more attractive. Note that the results at larger t are more reliable since the contaminations from inelastic states are more suppressed. The calculation of phase shifts with larger statistics is in progress. In comparison to the empirical phase shifts, it is also interesting to study the effect of the heavier pion mass in this simulation ($m_\pi \simeq 146$ MeV).

6 $N\Omega$ system ($S = -3$ channel)

We show the results of $N\Omega$ interaction in ${}^5S_2$ channel. Shown in Fig. 8 is the central force $V_C(r)$ obtained at $t = 11 - 14$. It is found that the interaction is attractive at all distances. Note that no Pauli blocking effect is present between N and Ω. The potential is found to be stable against the change of t, which implies that the coupling to the two octet baryon systems are suppressed and higher-order terms in the velocity expansion are small. We calculate the corresponding phase shifts $\delta_0(k)$ and present them in the form of $k \cot \delta_0(k)/m_\pi$ as a function of $(k/m_\pi)^2$ in Fig. 9. The data are aligned almost linearly as is expected by the effective range expansion at low energies, where the intercept at $k^2 = 0$ corresponds to the inverse of the scattering length and the slope corresponds to the (half of) the effective range. While the statistical fluctuations are still large, the results imply that the scattering length is negative (in particle physics convention) and the system is bound (compared to the $N\Omega$ threshold). Such a strong attraction can be studied through the $N\Omega$ pair-momentum correlation in heavy-ion collision experiments [19].

7 Summary

We have presented the latest lattice QCD results for baryon interactions at nearly physical quark masses, $m_\pi \simeq 146$ MeV and $m_K \simeq 525$ MeV on a large lattice box $(96a)^4 \simeq (8.1\text{fm})^4$. Baryon forces have been calculated from NBS correlators in the (time-dependent) HAL QCD method. We have shown preliminary results for $\Xi\Xi$, NN and $N\Omega$ interactions.

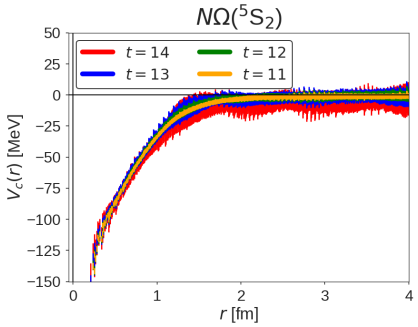

Figure 8. $N\Omega$ central force $V_C(r)$ in ${}^5S_2$ channel obtained at $t = 11 - 14$.

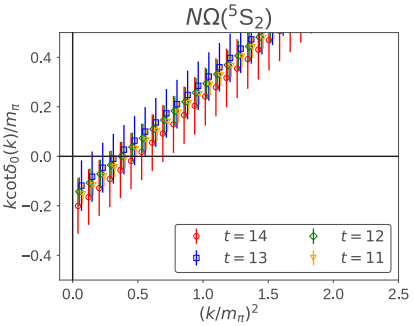

Figure 9. $k \cot \delta_0(k)/m_\pi$ in $N\Omega({}^5S_2)$ channel obtained at $t = 11 - 14$.

In the $\Xi\Xi({}^1S_0)$ channel, a strong attraction is obtained, although it is not strong enough to form a bound state. In the $\Xi\Xi$ (${}^3S_1$-${}^3D_1$) channel, the strong repulsive core exists in the central force. Tensor force is found to be weak and have an opposite sign compared to the NN tensor force. For NN forces, the strong tensor force is clearly obtained. Repulsive cores as well as mid- and long-range attractions have been observed in central forces in both ${}^1S_0$ and ${}^3S_1$-${}^3D_1$ channels, where repulsive core in $NN({}^1S_0)$ is stronger than $\Xi\Xi({}^1S_0)$. In the $N\Omega({}^5S_2)$ channel, the interaction is found to be attractive at all distances and a bound state (compared to the $N\Omega$ threshold) is possibly formed. Strong attractions observed in $\Xi\Xi({}^1S_0)$ and $N\Omega({}^5S_2)$ can be best searched through pair-momentum correlations in heavy-ion collision experiments. The physical interpretations for these baryon interactions from the point of view of quark Pauli blocking effect, one-gluon exchange at short distance and one-boson exchange potentials at mid to long distance are discussed.

The analysis with increased statistics is in progress. In future, it is also important to study baryon interactions in parity-odd channel including spin-orbit forces [24] and three-baryon forces [25], all of which have a large impact to determine the EoS of dense matter based on lattice QCD [26].

Acknowledgments

We thank members of PACS Collaboration for the gauge configuration generation. The lattice QCD calculations have been performed on the K computer at RIKEN, AICS (hp120281, hp130023, hp140209, hp150223, hp150262, hp160211, hp170230), HOKUSAI FX100 computer at RIKEN, Wako (G15023, G16030, G17002) and HA-PACS at University of Tsukuba (14a-20, 15a-30). T.D. and T.H. are supported in part by RIKEN iTHES Project and iTHEMS Program. We thank ILDG/JLDG [27] which serves as an essential infrastructure in this study. This work is supported in part by MEXT Grant-in-Aid for Scientific Research (JP15K17667), SPIRE (Strategic Program for Innovative REsearch) Field 5 project, "Priority Issue on Post-K computer" (Elucidation of the Fundamental Laws and Evolution of the Universe) and Joint Institute for Computational Fundamental Science (JICFuS).

References

[1] T. Doi and T. Inoue, Nucl. Phys. News **27** (2017) no.1, 13.
[2] B. P. Abbott *et al.* [LIGO Scientific and Virgo Collaborations], Phys. Rev. Lett. **119** (2017) no.16, 161101 [arXiv:1710.05832 [gr-qc]].
[3] B. P. Abbott *et al.* Astrophys. J. **848** (2017) no.2, L12 [arXiv:1710.05833 [astro-ph.HE]].
[4] N. Ishii, S. Aoki and T. Hatsuda, Phys. Rev. Lett. **99** (2007) 022001 [nucl-th/0611096]; S. Aoki, T. Hatsuda and N. Ishii, Prog. Theor. Phys. **123** (2010) 89 [arXiv:0909.5585 [hep-lat]].
[5] Reviewed in S. Aoki *et al.* [HAL QCD Collaboration], Prog. Theor. Exp. Phys. **2012** (2012) 01A105 [arXiv:1206.5088 [hep-lat]].
[6] N. Ishii *et al.* [HAL QCD Coll.], Phys. Lett. B **712** (2012) 437 [arXiv:1203.3642 [hep-lat]].
[7] S. Aoki *et al.* [HAL QCD Coll.], Proc. Japan Acad. B **87** (2011) 509 [arXiv:1106.2281 [hep-lat]]. S. Aoki *et al.* [HAL QCD Coll.], Phys. Rev. D **87** (2013) 034512 [arXiv:1212.4896 [hep-lat]].
[8] T. Doi and M. G. Endres, Comput. Phys. Commun. **184** (2013) 117 [arXiv:1205.0585 [hep-lat]].
[9] T. Yamazaki, K. i. Ishikawa, Y. Kuramashi and A. Ukawa, Phys. Rev. D **92** (2015) 014501 [arXiv:1502.04182 [hep-lat]] and refereces therein.
[10] K. Orginos *et al.* [NPLQCD Collaboration], Phys. Rev. D **92** (2015) 114512 [arXiv:1508.07583 [hep-lat]] and refereces therein.
[11] E. Berkowitz *et al.* [CalLat Coll.], Phys. Lett. B **765** (2017) 285 [arXiv:1508.00886 [hep-lat]].
[12] T. Iritani *et al.* [HAL QCD Collaboration], JHEP **1610** (2016) 101 [arXiv:1607.06371 [hep-lat]].
[13] T. Iritani *et al.*, Phys. Rev. D **96** (2017) no.3, 034521 [arXiv:1703.07210 [hep-lat]].
[14] T. Iritani [HALQCD Collaboration], arXiv:1710.06147 [hep-lat]; S. Aoki, T. Doi and T. Iritani, arXiv:1707.08800 [hep-lat].
[15] S. Gongyo *et al.*, arXiv:1709.00654 [hep-lat].
[16] T. Doi *et al.*, PoS LATTICE **2016** (2017) 110 [arXiv:1702.01600 [hep-lat]]; N. Ishii *et al.*, PoS LATTICE **2016** (2017) 127 [arXiv:1702.03495 [hep-lat]]; K. Sasaki *et al.*, PoS LATTICE **2016** (2017) 116 [arXiv:1702.06241 [hep-lat]]; H. Nemura *et al.*, PoS LATTICE **2016** (2017) 101 [arXiv:1702.00734 [hep-lat]].
[17] N. Ishii *et al.*, in these proceedings; K. Sasaki *et al.*, in these proceedings; H. Nemura *et al.*, in these proceedings.
[18] F. Etminan *et al.* [HAL QCD Coll.], Nucl. Phys. A **928** (2014) 89 [arXiv:1403.7284 [hep-lat]].
[19] K. Morita, A. Ohnishi, F. Etminan and T. Hatsuda, Phys. Rev. C **94** (2016) no.3, 031901 [arXiv:1605.06765 [hep-ph]].
[20] K.-I. Ishikawa *et al.* [PACS Coll.], PoS LATTICE **2015** (2016) 075 [arXiv:1511.09222 [hep-lat]].
[21] T. Boku *et al.*, PoS LATTICE **2012** (2012) 188 [arXiv:1210.7398 [hep-lat]]; M. Terai *et al.*, IPSJ Transactions on Advanced Computing Systems, Vol.6 No.3 43-57 (Sep. 2013) (in Japanese); Y. Nakamura *et al.*, Comput. Phys. Commun. **183**, 34 (2012) [arXiv:1104.0737 [hep-lat]].
[22] J. Haidenbauer *et al.*, Eur. Phys. J. A **51** (2015) 2, 17 [arXiv:1412.2991 [nucl-th]].
[23] M. Oka, K. Shimizu and K. Yazaki, Nucl. Phys. A **464** (1987) 700.
[24] K. Murano *et al.* [HAL QCD Coll.], Phys. Lett. B **735** (2014) 19 [arXiv:1305.2293 [hep-lat]].
[25] T. Doi *et al.* [HAL QCD Coll.], Prog. Theor. Phys. **127** (2012) 723 [arXiv:1106.2276 [hep-lat]].
[26] T. Inoue *et al.* [HAL QCD Coll.], Phys. Rev. Lett. **111** (2013) 112503 [arXiv:1307.0299 [hep-lat]]; T. Inoue [HALQCD Coll.], PoS INPC **2016** (2016) 277 [arXiv:1612.08399 [hep-lat]].
[27] `"http://www.lqcd.org/ildg"`, `"http://www.jldg.org"`